

**SEGMENTATION OF MULTISEQUENCE  
MEDICAL IMAGES USING RANDOM  
WALKS ALGORITHM AND ROUGH SETS  
THEORY**

by

**LIM KHAI YIN**

**Thesis submitted in fulfillment of the requirements  
for the degree of  
Doctor of Philosophy**

**July 2017**

## ACKNOWLEDGEMENT

First of all, my sincere gratitude to my supervisor, Professor Dr. Mandava Rajeswari from the School of Computer Sciences of Universiti Sains Malaysia, for her commitment of guiding throughout the completion of this thesis. Through the consistent supervision provided in this research, her guidance, valuable advice, and earnest propulsion has inspired me the passion on research.

Besides that, I wish to express my love and appreciation to my parents, Lim Soo Tick and Goh Bee Teen, my two sisters, Lim Khai Yee and Lim Khai Han, and my husband, Eric Kong Kok Wah, who have been my pillar of strength that has pushed me through. I could not have completed this study without their encouragement and support.

I would like to thank the School of Computer Sciences, USM, and Ministry of Higher Education for providing the grant of "Spatially aware Clustering Models for Multispectral Image Segmentation" with the grant number 1001/PKOMP/817067, and MyBrain15 scholarship, respectively.

Finally, I would like to thank those who have helped in any respect during my research, especially my lab mates Anusha Achuthan, Mogana Vadiveloo, administrative assistant from the School of Computer Sciences, Sheela Muniandy and many others whom the names I did not mention here.

## TABLE OF CONTENTS

ACKNOWLEDGEMENT .....	ii
TABLE OF CONTENTS.....	iii
LIST OF TABLES .....	vii
LIST OF FIGURES .....	viii
LIST OF ABBREVIATIONS .....	xiii
ABSTRAK .....	xv
ABSTRACT .....	xvii

### CHAPTER - 1 INTRODUCTION

1.1	Background.....	1
1.2	Medical Image Segmentation .....	3
	1.2.1 Multisequence Medical Images .....	3
	1.2.2 Challenges in Medical Image Segmentation .....	5
1.3	Problem Statement.....	7
	1.3.1 Information Modelling.....	8
	1.3.2 Information Fusion .....	9
	1.3.3 Extraction of Visual Object with Ambiguous Boundary .....	10
1.4	Research Objectives.....	11
1.5	Research Scope .....	11
1.6	Research Contributions.....	11
1.7	Thesis Outline .....	12

### CHAPTER - 2 LITERATURE REVIEW

2.1	Introduction.....	14
2.2	Multisequence Image Segmentation .....	14
	2.2.1 Vectorial Processing .....	17
	2.2.2 Sequential Processing .....	18
	2.2.3 Marginal Processing .....	19
	2.2.3(a) Pixel Level Image Fusion.....	20
	2.2.3(b) Feature Level Image Fusion.....	22
	2.2.3(c) Decision Level Image Fusion.....	24
	2.2.3(d) Discussion .....	25

2.3	Processes in Feature Level Fusion.....	27
2.3.1	Information Modelling.....	27
2.2.1(a)	Clustering Approaches .....	29
2.2.1(b)	Region based Approaches .....	31
2.2.1(c)	Discussion .....	39
2.3.2	Information Fusion using Primitive Methods.....	40
2.3.3	Extraction of Visual Object with Ambiguous Boundary .....	42
2.4	Summary and Direction .....	48

**CHAPTER - 3 THEORETICAL BACKGROUND: RANDOM WALKS  
ALGORITHM AND ROUGH SETS THEORY**

3.1	Introduction.....	51
3.2	Random Walks Algorithm .....	51
3.3	Random Walks in Image Segmentation.....	55
3.3.1	Edge Weights.....	56
3.3.2	Combinatorial Dirichlet Problem.....	56
3.3.3	System of Linear Equations .....	58
3.4	Rough Set Theory .....	62
3.4.1	Rough Membership Function .....	63
3.5	Summary .....	64

**CHAPTER - 4 MULTISEQUENCE IMAGE SEGMENTATION  
FRAMEWORK**

4.1	Introduction.....	65
4.2	Proposed Framework .....	65
4.2.1	Dataset .....	68
4.2.2	Evaluation Methods .....	71
4.3	Summary .....	73

**CHAPTER - 5 SEGMENTATION USING THE MODIFIED RANDOM  
WALKS: HOMOGENEITY- AND OBJECT-FEATURE  
BASED RANDOM WALKS (HORW)**

5.1	Introduction.....	74
5.2	Proposed Algorithm: Homogeneity- and Object-feature Based Random Walks (HORW) .....	74
5.2.1	Homogeneity-based Weighting Function .....	75

5.2.2	Object-feature Based Affinity.....	79
5.3	Experiments.....	82
5.3.1	Experiment I.....	82
5.3.1(a)	Experiments on Sensitivity of the Locations of Seeds.....	84
5.3.2	Experiment II.....	90
5.4	Summary.....	98

**CHAPTER - 6 INFORMATION THEORETIC ROUGH SETS FOR VISUAL OBJECT EXTRACTION**

6.1	Introduction.....	99
6.2	ITRS in Image.....	99
6.3	Proposed Methodology: ITRS Segmentation.....	103
6.4	Experiment.....	108
6.5	Summary.....	115

**CHAPTER - 7 MULTISEQUENCE IMAGE SEGMENTATION USING THE PROPOSED FRAMEWORK**

7.1	Introduction.....	117
7.2	Prior Studies Concerning Multisequence Brain Tumour Segmentation.....	117
7.3	Methodology.....	124
7.3.1	Step 0: Image selection.....	125
7.3.2	Step 1: Segmentation using HORW.....	129
7.3.3	Step 2: Probability Maps Fusion.....	132
7.3.3(a)	Variance Ratio.....	132
7.3.3(b)	Modified Variance Ratio.....	134
7.3.3(c)	Overview of the Fusion Approach.....	138
7.3.4	Step 3: Visual Object Extraction.....	140
7.4	Experimental Results.....	141
7.4.1	Comparison between the Proposed Weighted Averaging and Other Averaging Methods.....	142
7.4.2	Parameter Setting.....	146
7.4.3	Results of Brain Tumour Segmentation.....	148
7.5	Summary.....	156

**CHAPTER - 8 CONCLUSION AND FUTURE WORK**

8.1 Introduction..... 158  
8.2 Conclusion ..... 158  
8.3 Limitations and Recommendations for Further Research..... 161

**REFERENCES..... 162**

**APPENDIX**

Appendix A PRINCIPAL COMPONENT ANALYSIS (PCA) IMAGE FUSION  
..... 183

**LIST OF PUBLICATIONS**

## LIST OF TABLES

		<b>Page</b>
Table 2.1	Difference between Boundary- and Region-based Methods.	28
Table 3.1	Generations of the Laplacian Graph.	60
Table 4.1	MICCAI Brain Tumour Dataset Provided in Multimodal Brain Tumour Segmentation Challenge (MICCAI, 2013).	69
Table 5.1	Comparison of DICE between the Conventional (CRW) and the HORW using images in Figure 5.5.	86
Table 5.2	Dataset with its preselected slices	91
Table 6.1	The Average Results of Using the Different Evaluation Matrices on the Different Comparative Approaches and the Proposed ITRS Otsu and ITRS ME.	113
Table 7.1	Summary of Multisequence Brain Tumour Segmentation Methods.	119
Table 7.2	Signal Response for Edema and Tumour	128
Table 7.3	Selected Images with Tumour for Each Case.	129
Table 7.4	Values for the Inputs.	136
Table 7.5	Comparisons of the average RMSE using Weighted averaging (wAV), Averaging (AV), and PCA Fusion Methods.	145
Table 7.6	Segmented Results using the Proposed Frameworks on HG Cases.	151
Table 7.7	Segmented Results using the Proposed Frameworks on LG Cases.	151

## LIST OF FIGURES

		Page
Figure 1.1	Visual objects perceived by human vision.	1
Figure 1.2	The different sequences of MRI brain tumour image that show white matter, grey matter, cerebrospinal fluid (CSF), and tumour regions in (a) FLAIR, (b) T1, (c) T1-contrast, and (d) T2. Image (e) is the tumour gold standard.	5
Figure 1.3	Example of the partial volume effect (b) of the actual ideal object (a) (Soret et al., 2007).	6
Figure 1.4	Examples of intensity inhomogeneity caused by (a) the imaging scanner (Vovk et al., 2007) and (b) the echoic properties of multiple tissues in a brain tumour image.	7
Figure 2.1	Taxonomy of approaches or techniques in multisequence image segmentation. Contributions will be made respectively on random walks algorithm, weighted averaging method, and rough sets theory in each of the processes under feature level fusion.	16
Figure 2.2	Vectorial processing.	18
Figure 2.3	Sequential processing.	19
Figure 2.4	Marginal processing.	20
Figure 2.5	Pixel level image fusion.	20
Figure 2.6	Feature level image fusion.	22
Figure 2.7	Decision level image fusion.	24
Figure 2.8	Medical image segmentation approaches.	29
Figure 3.1	Random walker.	52
Figure 3.2	Circuit network.	53
Figure 3.3	Weighted graph.	56
Figure 3.4	Illustration of the approach of segmentation with two different labelled seeds. (a) and (b) show the probability of each vertex first reaches $s_1$ and $s_2$ , respectively, (c) shows the segmented result based on Eq. (3.16).	61
Figure 3.5	Graphical illustration of the set approximations.	63



Figure 3.6	Rough membership function.	64
Figure 4.1	The general framework of multisequence image segmentation.	66
Figure 4.2	Example of the gold standard provided by the BRATS datasets to show the visual object, tumour core region (region within the red contour) and edema region (region between the red and yellow contours).	70
Figure 4.3	Sample images with its gold standards provided in MICCAI dataset (MICCAI, 2013).	71
Figure 4.4	Sets indicating the TP, FP, FN, and TN.	72
Figure 5.1	Neighbourhood pixels with the different $R$ .	75
Figure 5.2	Eigenvectors with increasing radius, $R$ (Cour et al., 2005).	76
Figure 5.3	The probability maps of the left synthetic images (a) speckle noise (b) gradient image using the conventional, $(w_{ij})$ and the proposed homogeneity-based weighting function, $(w_{ijg})$ respectively.	78
Figure 5.4	(a) Original image with the predefined seeds (green star and blue dots are used to represent the foreground and background, respective). (b) The estimated probability image $[0, 1]$ .	81
Figure 5.5	Representative results using the CRW and the proposed HORW based on the limited user inputs (ROI in green and background in blue).	83
Figure 5.6	Mean DICE of CRW and HORW using images in Figure 5.5.	87
Figure 5.7	Mean TPF of the 10 experiments for each image (a-g) in Figure 5.5 using CRW and HORW.	87
Figure 5.8	Mean FPF of the 10 experiments for each image (a-g) in Figure 5.5 using CRW and HORW.	87
Figure 5.9	Mean TNF of the 10 experiments for each image (a-g) in Figure 5.5 using CRW and HORW.	88
Figure 5.10	Mean FNF of the 10 experiments for each image (a-g) in Figure 5.5 using CRW and HORW.	88
Figure 5.11	Misclassification rates of the tested images in Figure 5.5 using the CRW and HORW.	89

Figure 5.12	An example of the multisequence brain tumour image ("Medical Image Computing and Computer Assisted Intervention (MICCAI), Multimodal Brain Tumor Segmentation," 2012; MICCAI, 2013).	91
Figure 5.13	Sample images with the delineated tumour region. Region delineated in red represents the gold standard, while blue and green are regions delineated using HORW and CRW, respectively.	92
Figure 5.14	Box and whisker plot displays the five-point summary.	92
Figure 5.15	Box plot showing mean DICE using different segmentation methods for Case1.	93
Figure 5.16	Box plot showing mean DICE using different segmentation methods for Case2.	93
Figure 5.17	Box plot showing mean DICE using different segmentation methods for Case3.	93
Figure 5.18	Box plot showing mean DICE using different segmentation methods for Case4.	94
Figure 5.19	Box plot showing mean DICE using different segmentation methods for Case5.	94
Figure 5.20	Box plot showing mean DICE using different segmentation methods for Case6.	94
Figure 5.21	Sample images from Case 3 and Case 6 with its gold standard.	96
Figure 5.22	Average TPF of the six datasets using the different methods.	96
Figure 5.23	Average FPF of the six datasets using CRW, HORW, and GrowCut.	97
Figure 6.1	Proposed methodology, ITRS thresholding (ITRS Otsu and ITRS ME) segmentation.	104
Figure 6.2	Sample brain image with ambiguous boundary.	109
Figure 6.3	Experimental result of the rough object representation using the optimal pair of $(\alpha, \beta)$ .	110
Figure 6.4	Segmented results using the different clustering methods.	112
Figure 7.1	The overall scheme of the proposed multisequence brain tumor image segmentation.	125

Figure 7.2	The multisequence brain tumour images (BRATS_HG0011) and its gold standard.	127
Figure 7.3	Fractional-enhanced tumour in T1C image (BRATS_LG0013). The region within the delineated red ring represents the true tumour region as provided in the gold standard.	127
Figure 7.4	Sample intensity distribution using T1C for non-tumour tissue (white matter, grey matter, and CSF) and tumour tissue.	130
Figure 7.5	Samples of the generated probability maps using HORW.	131
Figure 7.6	The <i>obj</i> versus the <i>bg</i> regions.	133
Figure 7.7	Results obtained from the 100,000 validation test, where <i>true</i> shows $diffmw > diffw$ and <i>false</i> refers to $diffmw < diffw$ .	137
Figure 7.8	Bounding boxes, as provided by user.	139
Figure 7.9	General procedure of the proposed fusion approach.	140
Figure 7.10	Sample outputs of averaging and weighted averaging fusion using T1C and T2 in slice #83, BRATS_HG0003.	143
Figure 7.11	Sample outputs of averaging and weighted averaging fusion using T1C and T2 in slice #107, BRATS_LG0004.	144
Figure 7.12	Sample outputs of averaging and weighted averaging fusion using T1C and T2 in slice #107, BRATS_LG0008.	144
Figure 7.13	Average RMSE comparisons on the cases using wVA, AV, and PCA fusion methods.	146
Figure 7.14	Effect of step-size values on segmentation accuracy with ITRS Otsu over the different cases.	147
Figure 7.15	Effect of step-size values on segmentation accuracy with ITRS ME over the different cases.	148
Figure 7.16	Segmentation results for the different selected cases. Second column: input images. Third column: Overlaid tumour gold standard (yellow) and segmentation result (red) using the framework that uses ITRS Otsu.	150
Figure 7.17	Samples of HG and LG cases with the highest DICE using ITRS Otsu framework.	152
Figure 7.18	Samples of HG and LG cases with the lowest DICE using ITRS Otsu framework.	153

Figure 7.19	DICE Comparison using HG Data.	154
Figure 7.20	DICE Comparison using LG Data.	154
Figure 7.21	DICE comparison with the semi-automatic approaches.	155

## LIST OF ABBREVIATIONS

<b>MR</b>	Magnetic resonance
<b>ROI</b>	Region of interest
<b>TE</b>	Echo time
<b>TR</b>	Repetition time
<b>PD</b>	Proton density
<b>FLAIR</b>	Fluid attenuated inversion recovery
<b>T1C</b>	T1 contrast-enhanced
<b>CSF</b>	Cerebrospinal fluid
<b>PCA</b>	Principal component analysis
<b>DWT</b>	Discrete Wavelet transform
<b>DCxWT</b>	Daubechies complex wavelet transform
<b>DRT</b>	Discrete Ripplet Transform
<b>PET</b>	Positron emission tomography
<b>CT</b>	Computed tomography
<b>ICM</b>	Iterated conditional modes
<b>ITRS</b>	Information theoretic rough sets
<b>FCM</b>	Fuzzy C-mean
<b>MRSI</b>	MR spectroscopic imaging
<b>DWI</b>	Diffusion weighted imaging
<b>MPFCM</b>	Modified Possibilistic Fuzzy C-Means
<b>PWI</b>	Perfusion-weighted-imaging
<b>MARGA</b>	Multispectral Adaptive Region Growing Algorithm

<b>DCHS</b>	Harmony Search hybridized with FCM
<b>STIR</b>	Short Tau Inversion Recovery
<b>FGcM</b>	Fuzzy Generalized c-Means
<b>PGcM</b>	Possibilistic Generalized c-Means
<b>FDG</b>	F-2-fluoro-2-deoxyglucose
<b>MMSE</b>	Minimum mean square error
<b>HCM</b>	Hard c-means
<b>rcm</b>	Rough c-means
<b>GLCM</b>	Gray level co-occurrence matrices
<b>HORW</b>	Homogeneity- and Object-feature Based Random Walks

**SEGMENTASI IMEJ PERUBATAN BERBILANG JUJUKAN DENGAN  
MENGUNAKAN ALGORITMA PERJALANAN RAWAK DAN TEORI SET  
KASAR**

**ABSTRAK**

Segmentasi imej Magnetic Resonance (MR) merupakan satu tugas klinikal yang mencabar. Selalunya, satu jenis imej MR tidak mencukupi untuk memberikan maklumat yang lengkap mengenai sesuatu tisu patologi atau objek visual dari imej. Akibatnya, pakar radiologi sering menggabungkan imej berbilang jujukan pesakit untuk mengesahkan lokasi, perlanjutan, prognosis dan diagnosis sesebuah objek. Terdapat dua cabaran dalam segmentasi imej perubatan. Salah satunya adalah sempadan kabur yang muncul di antara objek dan rantau jirannya, dan cabaran yang lain adalah intensiti ketidakhomogenan yang muncul pada sesuatu rantau. Oleh itu, tesis ini memberi tumpuan kepada bagaimana segmen imej perubatan berbilang jujukan dapat dilaksanakan dengan berkesan. Tesis ini mencadangkan satu model marginal yang mengintegrasikan data dan pengetahuan domain ke dalam segmentasi imej MR berbilang jujukan. Model marginal adalah satu pendekatan yang memproses setiap turutan imej secara individu diikuti oleh gabungan untuk segmentasi. Kajian ini membahagikan model marginal kepada tiga modul, iaitu (i) pemodelan maklumat, (ii), penggabungan maklumat, dan (iii) pengekstrakan objek visual. Algoritma yang diubahsuai dan konsep baru dalam konteks pemrosesan imej telah dicadangkan dalam setiap modul untuk meningkatkan ketepatan segmentasi. Dalam modul pertama, algoritma perjalanan rawak digunakan untuk memodelkan maklumat imej. Disebabkan sempadan yang kabur dan ketidakhomogenan intensiti

yang muncul dalam imej, terma tambahan yang berasaskan komponen kehomogenan homogeneity dan ciri objek telah ditambah ke dalam fungsi pemberatan algoritma perjalanan rawak. Dalam modul kedua, kaedah pemurataan berpemberat telah digunakan untuk menggabungkan maklumat daripada jujukan imej yang berbeza. Kedua-dua pengetahuan daripada data dan pengguna telah disepadukan untuk menentukan berat bagi setiap jujukan untuk penggabungan. Bagi modul yang terakhir, konsep set kasar teori maklumat telah digunakan untuk menangani isu sempadan kabur yang mungkin muncul di antara objek visual dan latar belakangnya untuk pengekstrakan objek. Pendekatan marginal yang dicadangkan telah diuji dengan menggunakan set tumor otak MICCAI dan prestasinya dibandingkan dengan kaedah yang lain. Eksperimen menunjukkan keputusan yang memberangsangkan, iaitu pendekatan yang dicadangkan mampu mengekstrak tumor otak dengan purata ketepatan 0.7 dan 0.63 DICE masing-masing bagi tumor gred tinggi dan rendah. Berbanding dengan kaedah automatik dan semi automatik lain yang memerlukan proses latihan dan pengawalan yang cermat, pendekatan yang dicadangkan mampu mengekstrak tumor otak walaupun dengan menggunakan pengetahuan pengguna yang asas mengenai sesuatu imej.



# **SEGMENTATION OF MULTISEQUENCE MEDICAL IMAGES USING RANDOM WALKS ALGORITHM AND ROUGH SETS THEORY**

## **ABSTRACT**

Accurate Magnetic Resonance (MR) image segmentation is a clinically challenging task. More often than not, one type of MRI image is insufficient to provide the complete information about a pathological tissue or a visual object from the image. As a result, radiology experts often combine multisequence images of a patient to verify the location, extension, prognosis and diagnosis of an object. There are mainly two challenges in medical image segmentation. One is ambiguous boundary that appears between an object and its neighbouring region, and the other is intensity inhomogeneity that appears within a region. Thus, this thesis focuses on how to effectively segment multisequence medical images despite these two main challenges. This thesis proposes a marginal model that integrates both data and domain knowledge into multisequence MR image segmentation. Marginal model is an approach that processes each sequence of images individually followed by fusion for segmentation. This study divides the marginal model into three modules, which are (i) information modelling, (ii), information fusion, and (iii) visual object extraction. Strengthened algorithms and new concepts in the context of image processing are proposed in each of these modules to enhance segmentation. In the first module, random walks algorithm is used to model the information of an image. Because of the ambiguous boundary and intensity inhomogeneity that appear within an image, extra terms related to homogeneity- and object feature- based components are added into the weighting function of random walks algorithm. In the second module, weighted averaging method is used to fuse information from the image

sequences. Both data information of an image as well as user knowledge are integrated to determine the weights for each sequence for fusion. As for the last module, the concept of information theoretic rough sets (ITRS) is utilized to address the issue of ambiguous boundary that may appear between the visual object and its background for object extraction. The proposed marginal approach is tested on MICCAI brain tumour dataset and the performance is compared with the other established methods. The experiments show promising results, with the proposed approach's ability to extract brain tumour with an average 0.7 and 0.63 DICE accuracy for high- and low-grade tumour, respectively. As compared to the other fully- and semi-automatic methods that require training and careful initialization processes, the proposed approach is able to extract the brain tumour with rudimentary user knowledge about the image.

# CHAPTER 1

## INTRODUCTION

### 1.1 Background

In image processing, the definition of segmentation can be perceived as the process of partitioning an image into non-intersecting regions. The goal of segmentation is to delineate or identify visual objects from the background. Here visual objects refer to objects that are perceived as distinguishable image components. The objects are inherently associated with regions,  $R_i$ , and the idea of segmentation may be explained as,  $R_1 \cup R_2 \cup \dots, R_n = \Omega$  and  $R_i \cap R_j = \emptyset$  for  $i \neq j$ , where  $\Omega$  is all pixels in an image and  $R_i \subset \Omega$ .

Human vision is able to extract visual objects from images naturally. In Figure 1.1 for instance, despite the fact that the homogeneity in terms of image properties such as pixel intensities or texture is questionable, human vision perceives the highlighted regions as visual object or a region of interest (ROI).

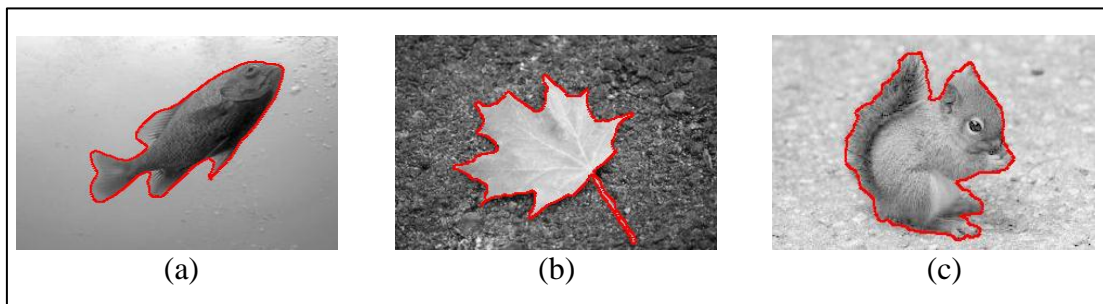


Figure 1.1: Visual objects perceived by human vision.

In computer vision, the main concept of segmentation techniques is based on the idea of homogeneity. Successful segmentation may be achieved if the objects

have homogenous image properties. In most real-world applications of image segmentation, however, one's biggest interest is to extract visual object from the image. Using methods that plainly offer homogeneity constraint on intensity are less meaningful in visual object extraction, especially when there are disconnected regions sharing similar intensities but belong to semantically different classes.

Image segmentation algorithms can be divided into three categories. Category 1 comprises algorithms that label individual pixels. Examples are thresholding- and clustering-based algorithms. Category 2 contains algorithms that label syntactic components. These include edge or boundary detection and corner detection. Category 3 comprises algorithms that label the regions. This covers all region-based segmentation algorithms. Algorithms in Category 1 are of generally non-contextual techniques, in which pixels are simply grouped together based on the intensity value of pixels without taking spatial information of the image into account. It may result in a large number of small segments, known as over-segmentation. These small segments may not have any visual meaning. To overcome this over-segmentation problem to some extent, noise smoothing or morphological post-processing methods can be imposed to remove the noisy fragments in the segmented image. Additionally, the segmentation technique itself can be modified to include a spatial component. Segmentation algorithms in Category 1, assign a label to each pixel at the end of segmentation, where they may not guarantee a connected segment. In practical applications, however, region labelling is necessary. For example, in medical image analysis, region needs to be delineated as the main interest lies in discriminating pathological tissue from healthy tissue (N. Sharma & Aggarwal, 2010). In such approaches, region labelling, which ensures continuity within the region, rather than pixel labelling, is more desirable.

## 1.2 Medical Image Segmentation

There are many applications to image segmentation, and one of the most common applications is in medical image analysis. There are mainly four major imaging techniques in medical imaging, which include X-ray imaging, magnetic resonance imaging (MRI), ultrasound imaging, and nuclear imaging (Toennies, 2012). Segmentation in medical imaging is often used to identify a structure that is especially useful in performing quantification of tissue volumes, diagnosis, localization of pathology, study of anatomical structures, treatment planning, and computer-integrated surgery (Pham et al., 2000).

### 1.2.1 Multisequence Medical Images

In the past few decades, MRI has been a well-known technique for its ability to characterize tissue. Strong magnetic fields and radio waves are used to produce images that are dependent on the hydrogen protons associated with water and fat in the body. Echo time (TE) and repetition time (TR) are the two controls that determine tissue contrast, which results in multiple images with different contrast for the same structure. These images are often referred to as multisequence images. The popular MRI sequences are following (Hesselink et al., 2005):

**T1-weighted (T1):** Uses a short TR and short TE ( $TR < 1000\text{msec}$ ,  $TE < 30\text{msec}$ ). Fluid appears as hypointense (low signal intensity or dark).

**T2-weighted (T2):** Uses a long TR and long TE ( $TR > 2000\text{msec}$ ,  $TE > 80\text{msec}$ ). Fluid appears as hyperintense (high signal intensity or bright).

**Proton density (PD):** Uses a long TR and short TE. Fluid appears as hyperintense.

**Fluid attenuated inversion recovery (FLAIR):** In some cases, this sequence replaces the PD image. Fluid effect is suppressed in FLAIR.

**T1 contrast-enhanced (T1C):** In order to highlight the abnormal tissues, Gadolinium-based agents are injected before the scan. The contrast agents may increase the signal intensity on T1, known as T1 contrast-enhanced (T1C) images. Pathological tissues such as tumours will appear hyperintense due to the accumulation of the contrast agent.

Since multisequence images obtained from different excitation sequences provide different image intensity information for a given anatomical region, more information about a tissue can be deduced by jointly analyzing all the sequences. The different grey contrasts in multisequence images have facilitated medical experts to distinguish the tissues in medical images. For example, referring to Figure 1.2, given the knowledge about the tumour, which is the ROI in this case, the hyperintense signal intensity in T1C would be a good indication of tumour. It is however found that the hyperintense region in T1C alone does not always guarantee the true tumour region (Drevelegas & Papanikolaou, 2011). This is because some tumour regions may not be enhanced due to the protective blood brain barrier that prevents the contrast agent from reaching the extravascular space or to necrotic region that does not take up contrast (Vigneron et al., 2001). Thus, it is necessary to include additional information provided by the remaining sequence(s) to further approve and complement the region of tumour in T1C.

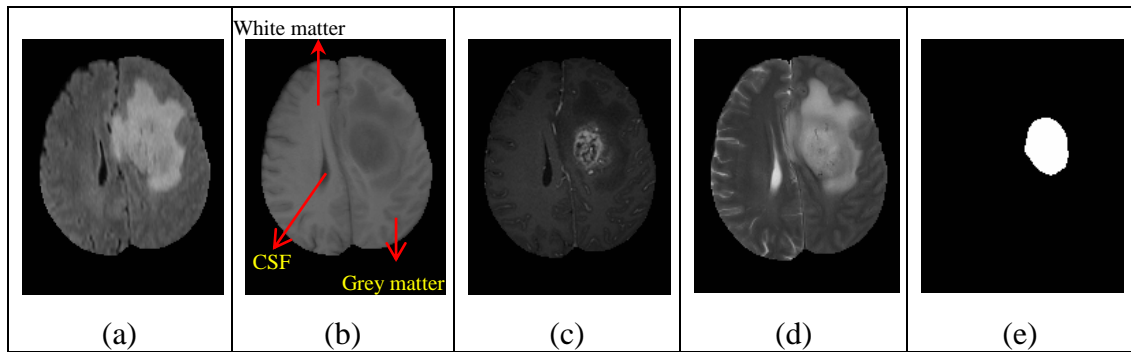


Figure 1.2: The different sequences of MRI brain tumour image that show white matter, grey matter, cerebrospinal fluid (CSF), and tumour regions in (a) FLAIR, (b) T1, (c) T1-contrast, and (d) T2. Image (e) is the tumour gold standard.

### 1.2.2 Challenges in Medical Image Segmentation

Challenges in medical image segmentation come from different aspects that mainly lie in the cognitive process and characteristic properties of an image.

#### (a) Cognitive Bias

Conventionally, the manual segmentation performed by radiology experts often induces joint analysis. In this analysis, images from different sequences are analyzed independently and later fused to demonstrate the correlations and attain the final visual object. This segmentation procedure practiced by medical experts is heuristic where the visual isolation is based on expert knowledge. Methodical rules extracted by expert's knowledge using information provided by the multisequence images are applied to delineate the visual object. Although this rule of thumb is reliable, its accuracy is a variable that depends on the proficiency of the expert and may be influenced by cognitive bias (Nodine & Mello-Thoms, 2000).

#### (b) Ambiguous Boundary

In addition to the complexity of combined analysis of multiple images, there are several other challenges to medical image segmentation. The most prominent of

these are ambiguous boundaries between the visual object and its neighbouring structures and the intensity inhomogeneities appearing within the image. The ambiguity of a region boundary could be a result of a gradual transition between the object and the background, which is a common phenomenon in medical images. One of the reasons for this ambiguity is due to the “partial-volume effect”. Partial-volume effect describes a phenomenon in which the appeared intensity values of images are different from their ideal values (Soret et al., 2007). These different projected intensities are often caused by the limited resolution of the imaging system that leads to dimmer and “spilled-out” region (Figure 1.3).

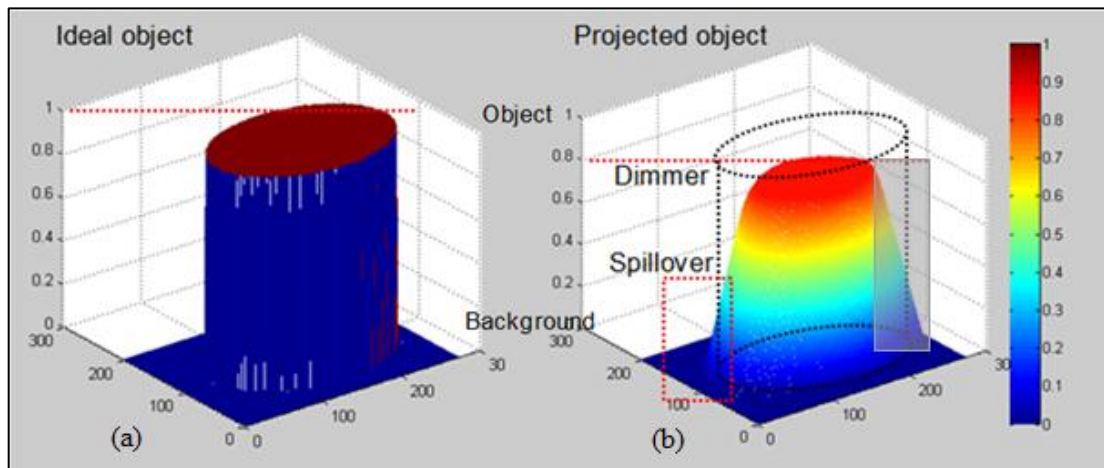


Figure 1.3: Example of the partial volume effect (b) of the actual ideal object (a) (Soret et al., 2007).

Figure 1.3(a) illustrates the ideal object, in which the pixels in object and background have distinct intensities. Whereas in Figure 1.3(b), the gradual transition region is indicated by the grey box. The pixel intensities in this transition region have a lower gradient thus definite segmentation is hard on this region.

### (c) Intensity Inhomogeneity

In medical imaging, intensity inhomogeneity can either be explained as the shading effect appears in the image, which is caused by the imaging scanner (Pham et al.,



2000); or the echoic properties, where a structure appears to have other tissues, such as fatty tissue, blood vessel and etc. that result in texture variation within a structure (Ding et al., 2012). Figure 1.4 demonstrates the intensity inhomogeneity in medical images.

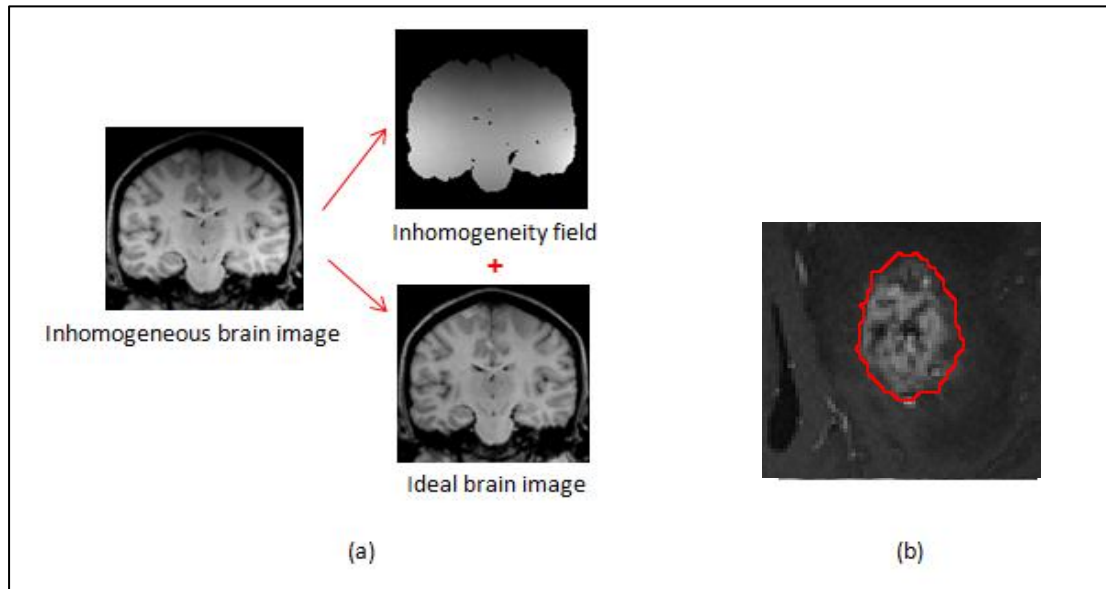


Figure 1.4: Examples of intensity inhomogeneity caused by (a) the imaging scanner (Vovk et al., 2007) and (b) the echoic properties of multiple tissues in a brain tumour image.

### 1.3 Problem Statement

The ultimate concern in this work is to effectively extract visual object by utilizing information from multisequence medical images without overlooking the inter-sequence dependencies between them.

This thesis adapts the marginal-based approach (notion borrowed from (Aptoula & Lefevre, 2007)) for multisequence image segmentation. Marginal-based approach segments ROI in each sequence of image independently and then aggregates the results to find the visual object. This thesis divides the approach into three modules, namely: (i) information modelling in each sequence using the random walks algorithm (ii) information fusion, and (iii) visual object extraction. From now

on in this thesis, ROI is used to refer to object in each sequence, while the term visual object represents object that is desired to be extracted from the fused image. The following subsections briefly describe the problems related to each of these modules.

### **1.3.1 Information Modelling**

This module uses random walks algorithm (Grady, 2006) to model image information. In random walks algorithm, image is treated as a weighted graph. The probability of a pixel belonging to each predefined seed generated by random walks algorithm represents the modeled information or the *appearance model* of an ROI. In spite of the numerous studies towards extending and enhancing the random walks algorithm for image segmentation (Baudin et al., 2012b; Eslami et al., 2013; Freedman, 2012; L. Guo et al., 2008; Onoma et al., 2014), the general issue, *sensitivity to seeds selection*, particularly to the locations of the seeds, has yet to be addressed. Thus, in order to enhance the algorithm, assuming the unchanged seeds, be it the locations or the number of seeds, the weighting function that constitutes the Laplacian matrix is pertinent to be studied. Though several studies (Dakua & Sahambi, 2009, 2011; Rzeszutek et al., 2009) have attempted various weighting functions in improving the random walks segmentation, the tangible properties of the proposed functions in the context of image segmentation were not being addressed. That is, the basis of the projected modifications did not take full advantage of the characteristics of the image itself. Hence, this study focuses on how to modify the weighting function of the random walks algorithm by utilizing the additional information provided by the image pixel intensities and their neighbourhood distribution to generate the appearance model of ROI.

### **1.3.2 Information Fusion**

In this module, the purpose of fusion is to aggregate the complementary information of the ROI from different sequences. Enhancing image quality such as generating fused image with better image resolution or visuality of certain region(s) is not as critical (Du et al., 2016). Thus here, the weighted averaging method that is able to produce fused image is deemed sufficient to compute a composite image with complementary information. The weighted averaging method enables the user to assign weights to different sequences. The role of a specific sequence can be emphasized or suppressed by respectively imposing higher and lower weights.

In general, the weight of each sequence can be estimated in three ways. The first method assumes that the source images (images to be fused) are captured at different exposure parameters, in which the significance of each image is based on its projected information, such as its luminance (Moumene et al., 2014). The second method requires a reference image, where the weights of the source images are estimated based on the variance of each source to the reference image (Ge et al., 2014). Whereas, the last method is based on the objectivity of the beholder, where the user arbitrarily determines the weights of each source images. Since the ROI appearance model in this work possess neither of the first two criteria, the prominence of one source over the other(s) can simply be determined based on the user's knowledge (Burt & Kolczynski, 1993; H. Lin et al., 2014). This heuristic approach, however, neglects the information carried within the image. Therefore, this thesis intends to investigate how to determine weights for each sequence of image by exploiting both image information as well as user's knowledge.

### 1.3.3 Extraction of Visual Object with Ambiguous Boundary

The fused image obtained by fusing the ROI modeled information from different sequences may not always have a sharp boundary but gradual transition between neighbouring regions. This phenomenon may be similar to the ambiguous boundary described in Section 1.2.2 (b). Therefore, methods that deal with ambiguity in region segmentation are preferred.

Typically, the approaches of segmenting images with ambiguity between regions can be categorized into three. This includes algorithms that exploit the concept of (i) fuzzy theory, (ii) rough sets theory, and (iii) transition region extraction followed by thresholding. In the fuzzy theory approach, the ambiguity between regions may be conveniently represented by probability that allows the degree of membership of a pixel to an object with value from 0 to 1. In rough sets theory approach, the uncertainty of knowledge is described in the aspect of “indiscernibility” (Walczak & Massart, 1999). Pixels that appear to be indiscernible in its property are grouped on the basis of perceived information. As for the thresholding based on transition region approach, segmentation is achieved by first extracting the transition region followed by thresholding the image based on the threshold value obtained from the transition region (Chao et al., 2006; Z. Li et al., 2014; Z. Li, D. Zhang, et al., 2011; Yan et al., 2003; Y. J. Zhang & Gerbrands, 1991).

It has been suggested that prior knowledge about the visual object could improve segmentation (Chen et al., 2012; Despotovi et al., 2015; Grady, 2012; Mesejo et al., 2015; Qingmao et al., 2006). The ability of the rough sets theory to address the ambiguity by grouping indiscernible objects based on the prior knowledge has made it an excellent research tool. Thus, this study explores on how to extract transition region accurately using the rough sets concept.

#### **1.4 Research Objectives**

The major objective of this research is to propose a framework to segment visual object using multisequence MR images. The sub-objectives are:

- i) To improve the segmentation in images with intensity inhomogeneity.
- ii) To improve the results of the multisequence images fusion.
- iii) To propose an algorithm to address ambiguous boundary region segmentation.

#### **1.5 Research Scope**

- i) In this work, only two sequences of multisequence brain tumour MR images are evaluated using the proposed framework.
- ii) The rules derivation in the ROI (tumour core that excludes edema region) identification is based on the common understanding (or experts' opinion) on the test datasets.

#### **1.6 Research Contributions**

The main contributions of this thesis are listed as follows:

- i) Developed a framework, which comprises three modules (information modelling, information fusion, and visual object extraction), to extract visual object from multisequence medical images. Contributions are made to each of these modules.
  - a. Random walks algorithm is modified to be more robust for seeds initialization and region inhomogeneity by adding additional terms into the weighting function of the algorithm.
  - b. A weighted fusion method that uses the information from both the image and user is proposed.

- c. The concept of ITRS is proposed to extract the ambiguous visual object from the fused information map.

## **1.7 Thesis Outline**

This thesis comprises eight chapters. The main content for each chapter is summarized as follows:

Chapter 2 presents the literature review on multisequence image segmentation, namely made up the common approaches used in segmenting images with multisequence information.

Chapter 3 discusses the theoretical background of the main segmentation approach used in this thesis, random walks algorithm. The analogy between the circuit network and random walks concept is illustrated. Besides that, rough sets theory is also covered in this chapter.

Chapter 4 presents the method and procedure used in segmenting the multisequence medical images. Dataset and the evaluation methods are also covered in this chapter.

Chapter 5 and 6 describe the modules involved in the proposed multisequence segmentation framework as an independent model. Different datasets were evaluated and compared to the existing methods closest to the proposed models.

Chapter 7 describes the experiment using the proposed framework to segment the multisequence brain tumour. The segmentation is evaluated and compared with the state of the art approaches.

Finally, Chapter 8 presents the conclusion that provides the achievements in this research. Limitations as well as the recommendations for further research are also discussed at the end of the study.

## CHAPTER 2

### LITERATURE REVIEW

#### 2.1 Introduction

In this chapter, topics related to multisequence image segmentation are reviewed. General approaches to multisequence image segmentation will be surveyed first followed by a comprehensive study on each of the modules in the proposed framework.

#### 2.2 Multisequence Image Segmentation

In medical image analysis, it is practically difficult to capture all the information regarding a desired tissue from a single sequence of image. With the use of multisequence images, it may be possible to obtain more discriminative information that is represented by different contrast of images. Images from multiple sequences can be observed for more accurate segmentation. Over the years, a large and growing body of studies have been investigating the segmentation of multisequence medical images (G. Lin et al., 2010; Llado et al., 2012; Murino et al., 2014; Pinto et al., 2015; N. Zhang et al., 2011). Generally, multisequence image segmentation can be achieved by using either supervised (classification) or unsupervised approaches (Hernández et al., 2011). In supervised algorithms, prior region information of the images is used to train the system; which means that when a new data is fed, the system is able to recognize the regions. In unsupervised approaches, on the other hand, segmentation is carried out without the training process. Several studies (Artan et al., 2014; Damangir et al., 2012; Demirhan et al., 2014; Y. Li et al., 2016; Murino et al., 2014; Ozer et al., 2010; K. Zhang et al., 2013) have contributed towards



supervised multisequence medical image segmentation. In these studies, information in the image is either represented by pixel values or by the extracted feature values from the images, which is treated as a vector for training and classification. Not counting the tedious learning process required by the supervised methods, such segmentation approaches are also more likely to generate results with fragmented regions when the spatial information of an image is usually ignored.

As for the unsupervised multisequence image segmentation, images are segmented without the aid of training sets. The three most common approaches are marginal-, vectorial-, and sequential-based processing approaches. In the marginal approach, each of the multisequence images is treated as an independent image for processing. The processed images, in either feature or segmented binary form, are then fused for visual object extraction. In vectorial processing, images in multisequence images are treated as a multi-dimension image with each pixel representing a vector values from different sequence of images. In sequential processing, information of one sequence of images is used on to another for final segmentation. Figure 2.1 presents the taxonomy of multisequence image segmentation approaches covered in this thesis. The grey boxes are approaches in multisequence image segmentation while the blue boxes are the three modules that fall under the marginal approach, specifically under feature level fusion. It should be noted that the algorithms discussed under this category are primarily applicable to a single sequence image. This taxonomy also serves as the underlying structure for this chapter.

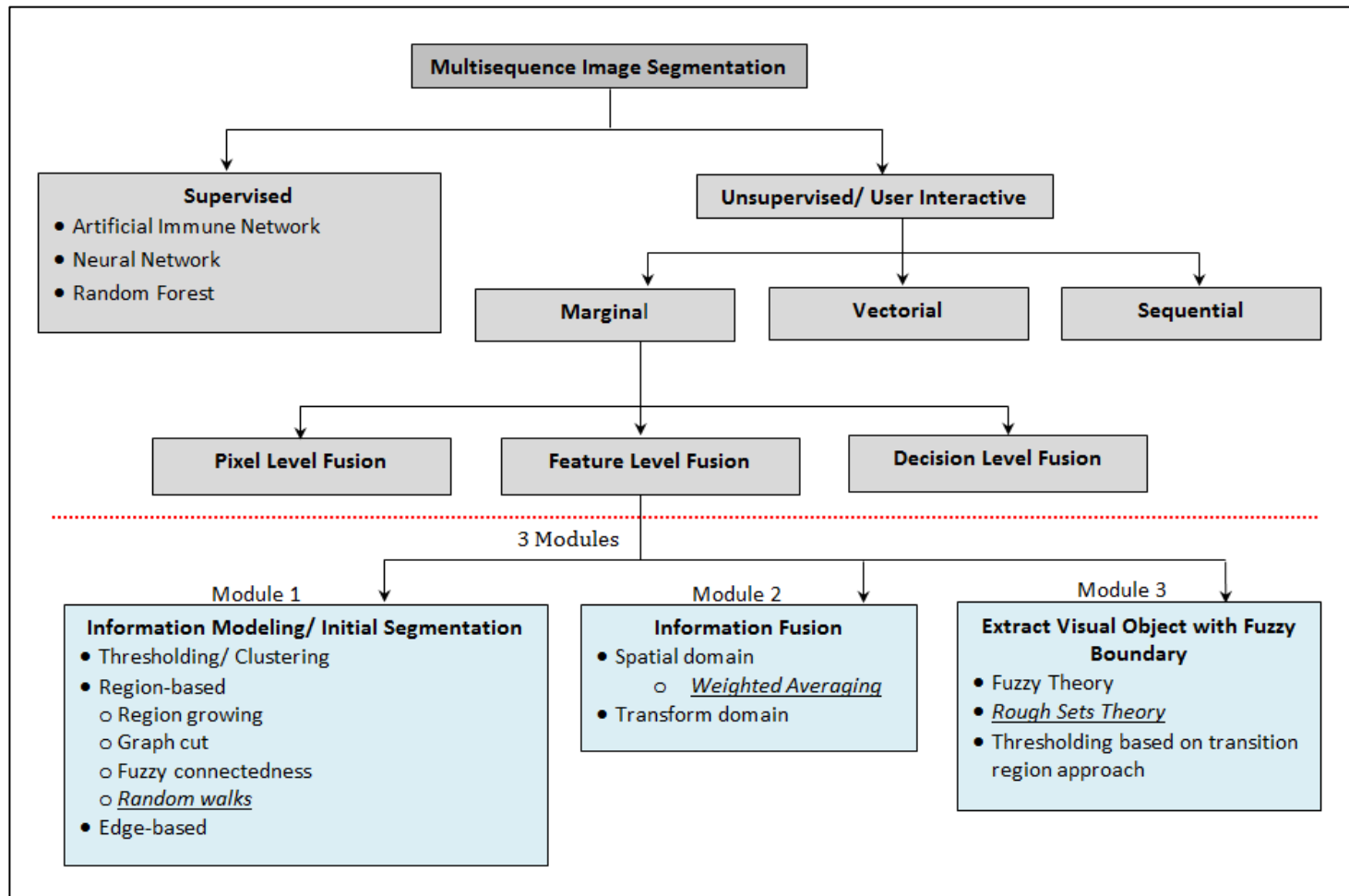


Figure 2.1: Taxonomy of approaches or techniques in multisequence image segmentation. Contributions will be made respectively on random walks algorithm, weighted averaging method, and rough sets theory in each of the processes under feature level fusion.

Gaps in each module under feature level fusion, particularly in the random walks algorithm, weighted averaging method, and visual object extraction using the rough sets theory are identified.

### **2.2.1 Vectorial Processing**

Vectorial processing is an approach towards multisequence segmentation, where pixels from the multisequence images are processed simultaneously as a vector during the clustering process. In G. Lin et al. (2012), multisequence MR images made up of the PD, T2-weighted and T1-weighted images were employed to segment normal and pathological tissues, grey matter, white matter, CSF and tumours. Each pixel information from the multisequence images is treated as a vector to identify the fuzzy edges and fuzzy similarity computation, which were later used to initialize the locations of the seeds for region growing. Chan et al. (2000) and Zhuge et al. (2006) employed vectorial information of the images in active contours algorithm and fuzzy connectedness, respectively. In the work conducted by Chan et al. (2000), Chan-Vese method of active contours algorithm was extended to vector based model to determine the boundary of the detected objects in multisequence images. In their work, each of the sequences was taken into account where the calculations in the scalar model were altered. For instance, the constant values in the Chan-Vese function were altered to constant vectors, consequently resulting in a change of the energy minimizing formula and Euler-Lagrange equations. Zhuge et al. (2006) extended the fuzzy connectedness from scalar scene domain to multisequence scene domain, at which the fuzzy affinity aspect was devised into a fully vectorial manner. Both the homogeneity-based and object-feature-based components of affinity were computed in the vectorial functional forms in order to extract affinity scene from the

multisequence images. Figure 2.2 depicts the segmentation using vectorial processing.

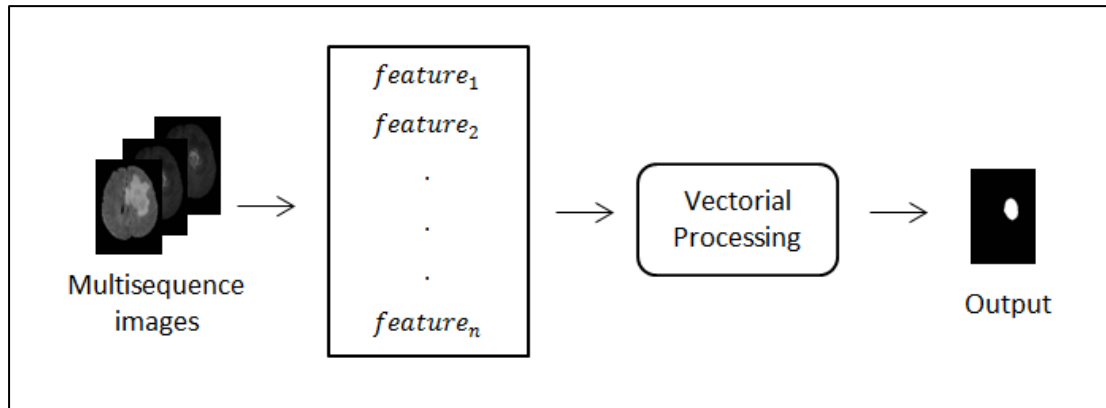


Figure 2.2: Vectorial processing.

### 2.2.2 Sequential Processing

In sequential-based processing, studies made use of one sequence's information of pixels on to another (Boudraa et al., 2000; Mandava et al., 2010; Ong et al., 2012). Instead of considering the whole image at once for object extraction, only certain region in an image is focused. For instance, in the study conducted by Boudraa et al. (2000), which in an attempt to automatically segment multiple sclerosis lesions using the multisequence MRI, PD weighted image was employed to extract the ROI for lesions segmentation. First of all, PD images were used to extract the intracranial contents of the brain followed by clustering using FCM to segment lesions and CSF. With the obtained lesions and CSF mask, T2 was exploited to further segment the lesions from T2 by performing FCM. Finally, the post-processing step based on the anatomical knowledge to discard the extra segmented regions was carried out.

Mandava et al. (2010) proposed to combine both the information of STIR (Short Tau Inversion Recovery) and T2 weighted images to segment the necrotic tissue in Osteosarcoma. STIR image was first segmented using the dynamic

clustering algorithm based on the Harmony Search hybridized with FCM (DCHS) for tumour extraction. The generated tumour mask was then multiplied with the corresponding T2 weighted image for necrotic segmentation. In which, the number of clusters was automatically identified using the DCHS algorithm. In the study done by Ong et al. (2012), T1 weighted and fluid-attenuated inversion recovery (FLAIR) sequences were used to segment white matter lesion. In the study, T1 images were used to perform the skull-stripping process using model-based level set approach and N3 inhomogeneity correction. The extracted skull-less mask of T1 was then applied on FLAIR to perform WML segmentation by using the proposed novel method of adaptively calculating the trimmed mean from the asymmetrical histogram. Figure 2.3 illustrates an example of the sequential processing involving two sequences.

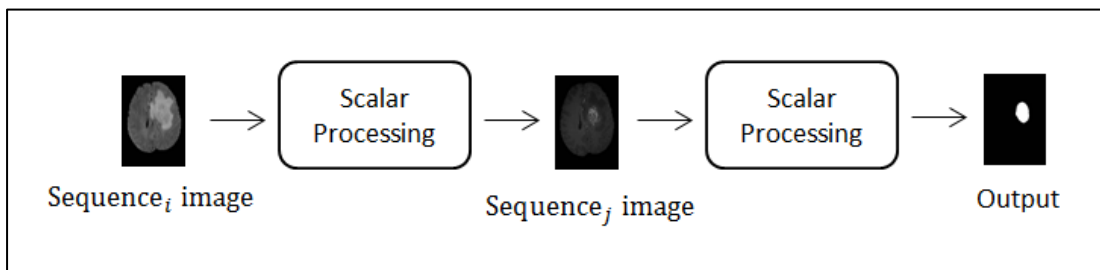


Figure 2.3: Sequential processing.

### 2.2.3 Marginal Processing

In marginal approach, fusion is performed to combine different information that is projected in different image sequence (Figure 2.4). In general, fusion can be carried out at three different processing levels (Pohl & Van Genderen, 1998), which are pixel level, feature level, and decision levels.

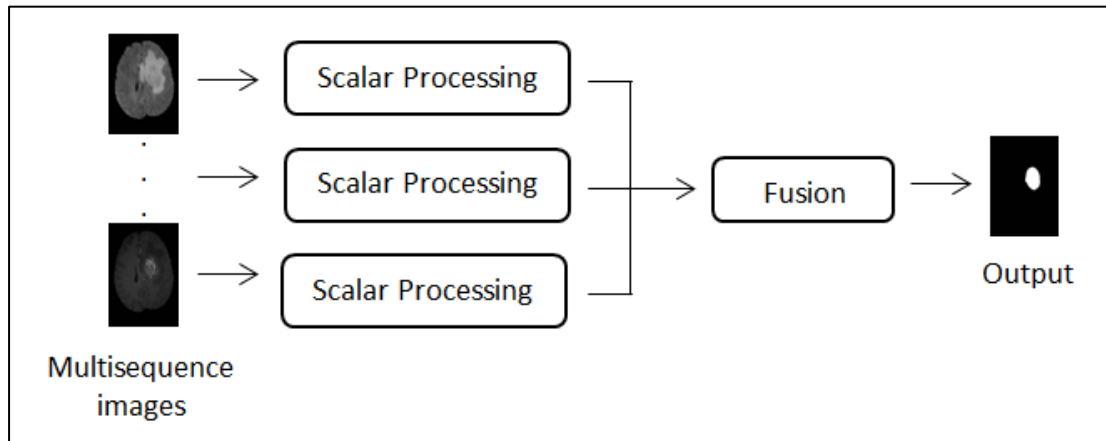


Figure 2.4: Marginal processing.

### 2.2.3(a) Pixel Level Image Fusion

Fusion at pixel level is the information fusion on pixel-by-pixel basis. This is the lowest level of image fusion. The fusion structure is depicted in Figure 2.5.

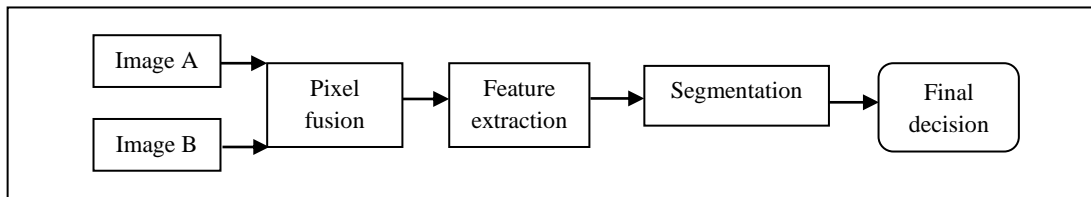


Figure 2.5: Pixel level image fusion.

Pixel level fusion combines images of the same scene, which are in the same dimension into a single image. The fused image may provide improved feature for better segmentation. Numerous studies have worked on pixel level image fusion in the past decades (Mishra & Palkar, 2015). Generally, pixel level fusion is carried out either in the original spatial domain or in the transform domain.

In the spatial domain, information of pixels from the source images is manipulated to form the fused image. Excluding color-based image fusion technique such as the intensity-hue-saturation fusion, principal component analysis (PCA) and primitive fusion are among the most common approaches in grey-level image fusion